Journal of
Nanoelectronics and Optoelectronics
Vol. 8, 1–5, 2013

Controlling Recombination Kinetics of Hybrid Nanocrystalline Titanium Dioxide/Polymer Solar Cells by Inserting an Alumina Layer at the Interface

S. Loheeswaran[1,2], K. Balashangar[1], J. Jevirshan[1], and P. Ravirajan[1,*]

[1] *Department of Physics, University of Jaffna, Sri Lanka*
[2] *Department of Physical Science, Eastern University, Sri Lanka*

This work focuses on improving the performance of hybrid titanium dioxide (TiO_2)/polymer solar cells by modifying the metal oxide-polymer interface using an alumina (Al_2O_3) layer. Optical absorption measurement shows that polymer uptake of TiO_2 electrodes is improved when the electrode is coated with an alumina layer. This may be due to the more basic nature of the alumina layer. Insertion of alumina coating on nanocrystalline TiO_2 increases both current density and open-circuit voltage of TiO_2/polymer devices, and so improves the overall efficiency by a factor of two. This is due to suppression of interfacial recombination of the carriers. The device with alumina coating shows external quantum efficiency of over 45% at the peak absorption of the polymer, and overall power conversion efficiency of over 1.4% under illuminations of intensity 70 mW/cm^2 with air mass 1.5 filter.

Keywords: Solar Cell, Photovoltaic Device, Titanium Dioxide, Polymer, Alumina, Recombination, Nanoparticles.

RESEARCH ARTICLE

1. INTRODUCTION

Composites of conjugated polymers with nanostructured metal oxides are promising material combinations for low-cost solar energy conversion. However, the performance of devices based on such structures is still limited by several factors, including inefficient exciton dissociation and interfacial charge recombination. One strategy to address this issue is to control the interfacial charge recombination by modifying the physical properties of the interface.

The device performance of polymer solar cells depends on the sequential processes of charge dissociation, transport, and collection. The interfacial contact plays a central role in the charge collection. Control of the structure of inorganic materials on the nanometer scale is currently attracting extensive interest in relation to dye-sensitized solar cells.[1–5] A range of fabrication procedures has been developed for the fabrication of nanoporous metal-oxide films comprising continuous networks of inorganic nanoparticles. The metal/organic interface thus plays an essential role in determining the overall device performance of the photovoltaic cell, and inserting an interfacial layer can dramatically alter the interface properties. Charge selectivity at the interfaces is crucial to ensure effective charge extraction, because it blocks the charge carrier from flowing in the unfavored direction. It has been reported that the conformal growth of insulating overlayers on the surfaces of nanoporous films, as shown in Figure 1, may be an important approach to achieving high efficiency in dye-sensitized solar cells.[1–5] Palomares et al. reported that the recombination half-time for the coated film is longer than for the uncoated film, indicating that the Al_2O_3 provides a kinetic barrier to charge recombination to dye cations.[7]

It was also reported that Al_2O_3-coated TiO_2 porous films were used to fabricate solid-state dye-sensitized solar cells using CuI as a hole conductor. Photovoltage transient measurements showed that the Al_2O_3 interlayer slowed down the interfacial recombination of electrons in TiO_2 with holes in CuI by forming a potential barrier at the TiO_2/CuI interface.[5]

It was found that the barrier reduces the recombination of photo injected electrons to both dye cations and the oxidized redox couple. This observed retardation can be attributed primarily to two effects: passivating almost completely surface trap states in TiO_2 that are able to inject electrons into acceptor species, and slowing down by a factor of three to four the rate of interfacial charge transfer from conduction-band states.[10]

Although considerable work has been done in dye-sensitized solar cells with a view to modifying the interface by an ultra-thin alumina layer, there has been no

*Author to whom correspondence should be addressed.

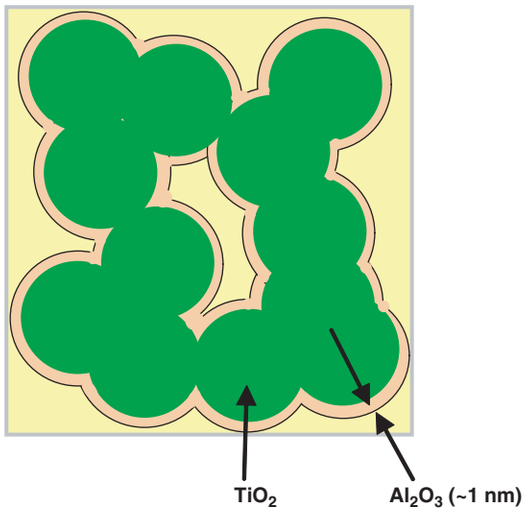

Fig. 1. Schematic representation of the TiO_2 nanoparticles, coated with an alumina overlayer.

similar work done in hybrid polymer/metal oxide solar cells. This work addresses the effect of alumina coating of TiO_2 nanoparticles on the performance of hybrid TiO_2/polymer solar cells.

2. EXPERIMENTAL DETAILS

The TiO_2 electrodes, consisting of an ITO-coated glass substrate with a 50 nm-thick dense TiO_2 layer and a $\sim$100 nm-thick nanoporous TiO_2 layer, were prepared as described in Refs. [6–8]. Hybrid polymer/TiO_2 structures with interface modification were achieved by first heating the films at 110 °C for 10 minutes to remove surface water, followed by dipping in a 1 mM precursor solution of aluminum tri-*sec*-butoxide in dry 2-propanol (IPA) for 20 minutes under ambient conditions. Samples were then rinsed in IPA and dried in nitrogen gas, followed by sintering at 435 °C for 20 minutes. Identical porous TiO_2 films without Al_2O_3 coating were subjected to similar heat treatment, rinsed in IPA solution and dried in nitrogen, and also sintered for the same duration as coated ones, in order to act as control structures. The precursor solution was heated to 60–70 °C prior to dipping the nanocrystalline film in it for 20 minutes, followed by dipping in N719 dye (Solaronix) solution and P3HT polymer (Merck Chemicals Ltd.) solution. A polymer layer approximately 50 nm thick was then spin-coated on to the dip-coated electrode. Optical absorbances of films were noted using a UV-VIS spectrometer (JASCO). The top contact electrode was made by thermal evaporation of Au using a thermal evaporator (Edwards E306) after deposition of a poly(ethylenedioxythiophene):polystyrene sulphonate (PEDOT:PSS) layer, as in Ref. [9].

The electrical characterization of the solar cells was carried out using a computer-controlled source measure unit (Keithley 2400) in dark and under 70 mW/cm^2 illuminations by using a solar simulator (SCIENCETECH) with an AM 1.5 filter. The external quantum efficiency measurement was also carried out using a calibrated 818-UV low-power photo-detector. A pulse laser (Big Sky Laser, 8 ns pulse width, 532 nm wavelength) was used for transient photovoltage measurements. The solar cell sample was irradiated through ITO, using the pulse laser at intensity 30 μJ at a wavelength of 532 nm. Photovoltage transients were recorded by connecting the cell directly to a digital oscilloscope (Tektronix, TDS1012B), as shown in Figure 2.

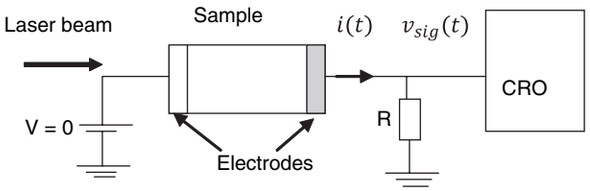

Fig. 2. Schematic diagram of photovoltage transient measurement set-up.

3. RESULTS AND DISCUSSION

Figure 3 shows the external quantum efficiency (EQE) spectra, measured in short-circuit current conditions, of a device with an alumina coating and its corresponding control. The figure shows that the peak EQE of the solar cell increases from 30% to 45% after inserting the alumina coating. As can be seen, at a peak of 525 nm in the figure, almost 45% of the incident photons lead to a current in the external circuit in the alumina-treated device while for its control device, 30% of the incident photons lead to a current in the external circuit at a peak of 510 nm. The higher external quantum efficiency of the device with alumina film may be attributed to the higher polymer uptake of alumina-treated nanoporous electrodes in comparison to the bare film, as shown in Figure 4. Higher polymer uptake

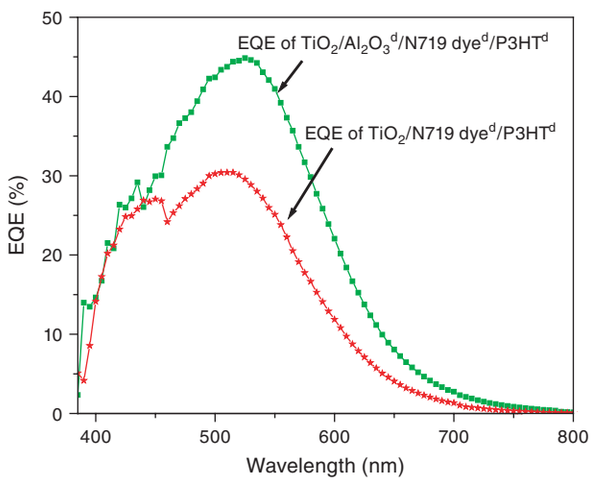

Fig. 3. External quantum efficiency spectra of the devices as prepared.

RESEARCH ARTICLE

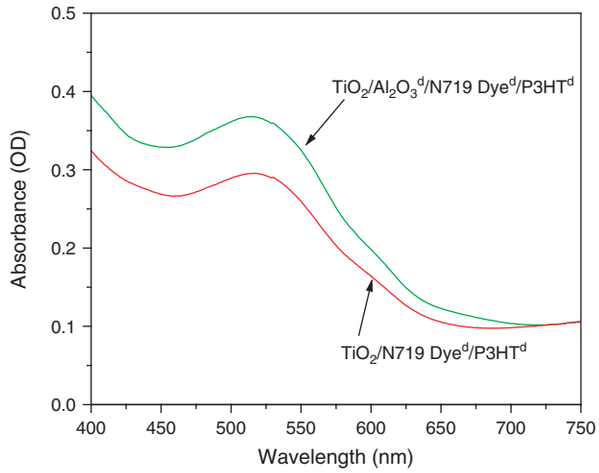

Fig. 4. UV-VIS optical absorption spectra of TiO_2 nanoporous films (100 nm thick) with and without alumina coating dipped in to N719 dye (0.3 mM) for two hours at room temperature, and into polymer (∼ 1 mg/ml) solutions for 18 hours at 120 °C.

of alumina-treated electrodes may be due to the more basic nature of the surface of the alumina layer.

Figure 5 shows the current–voltage characteristic for the alumina-coated device, and for its control. In general, the insulating alumina layer increases the open-circuit voltage from 0.37 V to 0.45 V, and short-circuit current density from 4.38 mA cm^{-2} to 6.30 mA cm^{-2}. The overall power conversion efficiency is thus increased from 0.7% to 1.4%. Due to better attachment of polymer on alumina-coated surfaces and the suppression of interfacial recombination, the number of charge carriers produced in the active layer reaching the top electrode is increased.

Figure 6 shows that the dark current is suppressed in devices with an Al_2O_3 layer. This prompted for transient

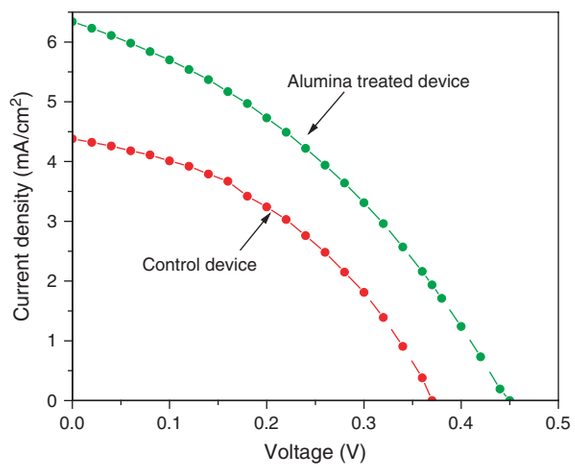

Fig. 5. *J–V* characteristics of a multilayer device (ITO/Dense TiO_2/PorousTiO_2/$Al_2O_3{}^d$/Dye^d/$P3HT^d$/$P3HT^s$/PEDOT:PSS/Au) with (green line) or without (red line) alumina coating under AM 1.5 solar spectrum irradiation (70 mW cm^{-2}, 1 sun). Superscripts d and s indicate dip and spin-coated layers, respectively

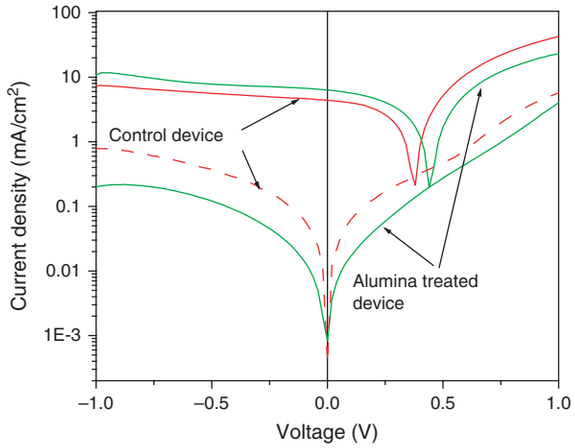

Fig. 6. Current density versus voltage characteristic of the alumina-coated and control devices under AM 1.5 (70 mW cm^{-2}) illumination (solid lines) and in dark (dashed line).

photovoltage measurement using pulse laser to find out the interfacial recombination kinetics. Since all the charges generated in the cell by the laser pulse recombine through the interface under open-circuit conditions, this measurement provides a direct investigation in to the effect of an Al_2O_3 layer on interfacial recombination.

Figure 7 compares the photovoltage transients of a cell fabricated with alumina-coated porous TiO_2 film to those of its control. Comparison of the absolute value of photovoltage in the transients of the two cells was not critical for the investigation into interfacial recombination. As such, two curves were normalized and compared over the uprising time and the decay life time of the photovoltage transients. Figure 7 shows that the photovoltage transients of both cells uprose quickly and then decayed in a single exponential way. The uprising time for the cell made from bare TiO_2 film is 2 μs, while it is 20 μs for the cell made from alumina-coated porous TiO_2 film. The uprising

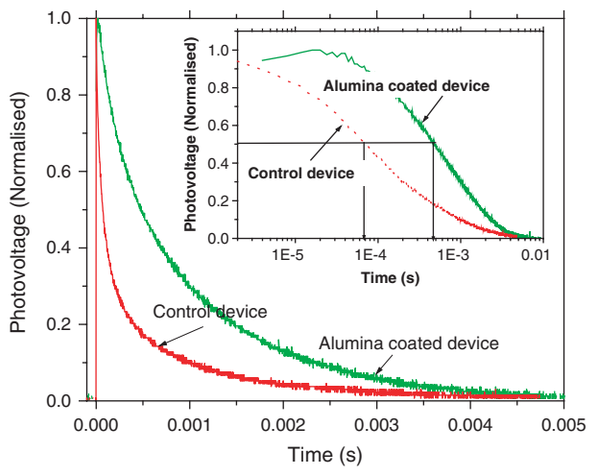

Fig. 7. Normalized photovoltage transients of the TiO_2/polymer device with (green line) and without (red line) Al_2O_3 coating films.

RESEARCH ARTICLE

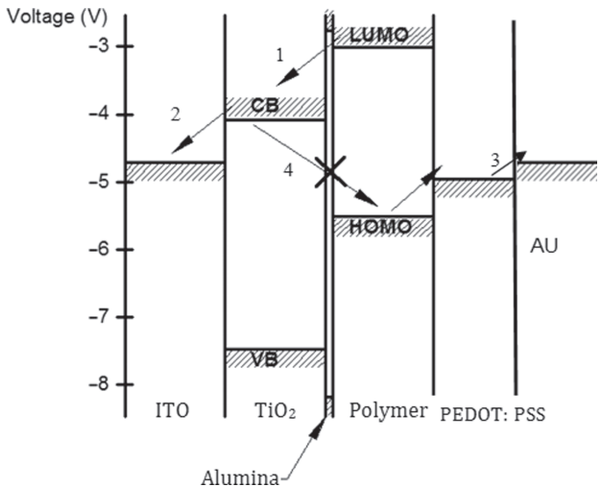

Fig. 8. Proposed electronic energy-level diagram for the ITO/dense TiO_2/porous TiO_2/Al_2O_3/P3HT/PEDOT:PSS/Au device, illustrating electron injection by tunneling (1) from the LUMO level of the photo-excited polymer through an ultra-thin alumina layer. The transferred electrons are collected (2) by the ITO electrode (2), while photo-generated holes are collected (3) by Au. The alumina layer suppresses the back electron transfer from TiO_2 to the polymer (interfacial recombination) (4).

time increases by an order of magnitude for the cell made from Al_2O_3-coated TiO_2 film in comparison with the control device. Thus, photo-injected electrons can move longer distances in a cell containing an Al_2O_3 interlayer. It is reasonable to consider the blocking function of this insulator interlayer in interfacial recombination. The lifetimes of the decays were calculated as 0.07 ms for the control cell, but 0.5 ms for the cell containing the Al_2O_3 coating. This shows direct evidence that an Al_2O_3 interlayer could slow down the interfacial recombination in a TiO_2/polymer device.

Concerning the interfacial energetic in a hybrid polymer/TiO_2 structure, the alumina overlayer on the TiO_2 nanoparticles suppresses interfacial recombination, as illustrated in Figure 8. The wideband gap of Al_2O_3 ensures the formation of a sufficiently large potential barrier on the surface of the TiO_2. Therefore, an Al_2O_3 layer could passivate the surface of TiO_2 and confine the movement of injected electrons in the TiO_2 phase.

4. CONCLUSION

A workable approach for the enhancement of the photovoltaic performance of hybrid nanocrystalline titanium dioxide/polymer solar cells through interface modification by means of an alumina layer was presented. This provides a design strategy to improve the performance of this type of cell. The Al_2O_3 coating serves multiple functions—as physical barrier layers for charge recombination reactions to affect the photo induced charge transfer at the interface, as a means of passivation of TiO_2 surface trap states, and to improve the exciton dissociation efficiency at the polymer/TiO_2 interface, as well as acting as a template for absorbance of polymer on nanoporous TiO_2 due to the more basic surface on the alumina-coated porous TiO_2 film. It has been found that alumina overlayer on TiO_2 nanoparticles increases short-circuit current density and open-circuit voltage, and hence increases the overall efficiency by a factor of two. The results of a study of photovoltage transients give clear evidence for the suppression of interfacial recombination by the insulating alumina layer, and better polymer uptake. We consider the ability of this alumina coating to modulate interfacial electron transfer dynamics and thereby improve the performance of TiO_2/polymer solar cells.

Acknowledgments: P. Ravirajan and K. Balashangar acknowledge the National Research Council (NRC) for financial assistance, and SL acknowledges the support of the Ministry of Higher Education for the HETC scholarship.

References and Notes

1. K. Tennakone, J. Bandara, P. K. M. Bandaranayake, G. R. R. A. Kumara, and A. Konno, *Jpn. J. Appl. Phys.* 40, L732 (**2001**).
2. G. R. R. A. Kumara, K. Tennakone, V. P. S. Perera, A. Konno, S. Kaneko, and M. Okuya, *J. Phys. D: Appl. Phys*. 34, 868 (**2001**).
3. E. Palomares, J. N. Clifford, S. A. Haque, T. Lutz, and J. R. Durrant, *Chem. Commun*. 14, 1464 (**2002**).
4. F. Li, H. Tang, J. Anderegg, and J. Shinara, *Appl. Phys. Lett*. 70, 1233 (**1997**).
5. X. T. Zhang, H. W. Liu, T. Taguchi, Q. B. Meng, O. Sato, and A. Fujishima, *Sol. Energy Mater. Sol. Cells* 81, 197 (**2004**).
6. P. Ravirajan, S. A. Haque, J. R. Durrant, D. Poplavskyy, D. D. C. Bradley, and J. Nelson, *J. Appl. Phys*. 95, 1473 (**2004**).
7. E. Palomares, J. N. Clifford, S. A. Haque, T. Lutz, and J. R. Durrant, *J. Am. Chem. Soc*. 125, 475 (**2003**).
8. P. Ravirajan, S. A. Haque, J. R. Durrant, D. Poplavskyy, D. D. C. Bradley, and J. Nelson, *Adv. Funct. Mater*. 15, 609 (**2005**).
9. P. Ravirajan, S. A. Haque, J. R. Durrant, S. J. P. Smith, J. M. Kroon, D. D. C. Bradley, and J. Nelson, *Appl. Phys. Lett.* 86, 143101 (**2005**).
10. F. F. Santiago, J. G. Cañadas, E. Palomares, J. N. Clifford, S. A. Haque, J. R. Durrant, G. G. Belmonte, and J. Bisquert, *J. Appl. Phys*. 96, 6903 (**2004**).
11. J. N. Clifford, E. Palomares, M. K. Nazeeruddin, M. Grätzel, J. Nelson, X. Li, N. J. Long, and J. R. Durrant, *J. Am. Chem. Soc*. 126, 5225 (**2004**).
12. A. Kay and M. Grätzel, *Chem. Mater*. 14, 2930 (**2002**).
13. G. R. A. Kumara, A. Konno, K. Shiratsuchi, J. Tsukahara, and K. Tennakone, *Chem. Mater*. 14, 954 (**2002**).
14. G. R. A. Kumara, S. Kaneko, M. Okuya, and K. Tennakone, *Langmuir* 18, 10493 (**2002**).
15. G. R. A. Kumara, A. Konno, G. K. R. Senadeera, P. V. V. Jayaweera, D. B. R. A. De Silva, and K. Tennakone, *Sol. Energy Mater. Sol. Cells* 69, 195 (**2001**).
16. B. O'Regan, D. T. Schwartz, S. M. Zakeeruddin, and M. Grätzel, *Adv. Mater*. 12, 1263 (**2000**).
17. B. O'Regan, F. Lenzmann, R. Muis, and J. Wienke, *Chem. Mater*. 14, 5023 (**2002**).
18. U. Bach, Y. Tachibana, J. E. Moser, S. A. Haque, J. R. Durrant, M. Grätzel, and D. R. Klug, *J. Am. Chem. Soc*. 121, 7445 (**1999**).
19. C. W. Tang, S. A. VanSlyke, and C. H. Chen, *J. Appl. Phys*. 65, 3610 (**1989**).
20. J. H. Burroughes, D. D. C. Bradley, A. R. Brown, R. N. Mark, K. Mackay, R. H. Friend, P. L. Burn, and A. B. Holmes, *Nature* 347, 539 (**1990**).

RESEARCH ARTICLE

21. G. Gastafsson, Y. Cao, G. M. Treacy, F. Klavetter, N. Colaneri, and A. J. Heeger, *Nature* 357, 477 **(1992)**.
22. N. C. Greenham, S. C. Moratti, D. D. C. Bradley, R. H. Friend, and A. B. Holmes, *Nature* 365, 628 **(1993)**.
23. S. Tasch, A. Niko, G. Leising, and U. Scherf, *Appl. Phys. Lett*. 68, 1090 **(1996)**.
24. I. D. Parker, *J. Appl. Phys*. 75, 1656 **(1994)**.
25. C. Adachi, S. Tokito, T. Tsutaui, and S. Saito, *Jpn. J. Appl. Phys*. 27, L713 **(1988)**.
26. C. Adachi, T. Tsutsui, and S. Saito, *Appl. Phys. Lett*. 57, 531 **(1990)**.
27. C. Hosokawa, H. Higashi, and T. Kusumoto, *Appl. Phys. Lett*. 62, 3238 **(1993)**.
28. Y. Ohmori, A. Fuji, M. Uchida, C. Morisbima, and K. Yoshino, *Appl. Phys. Lett*. 62, 3250 **(1993)**.
29. M. Berggren, O. Inganäs, G. Gustafsson, J. Rasmusson, M. R. Andersson, T. Hjertberg, and O. Wennerström, *Nature* 372, 444 **(1994)**.
30. Y. Ohmori, A. Fuji, M. Uchida, M. Yoshida, and K. Yoshino, *Jpn. J. Appl. Phys*. 34, 3790 **(1995)**.

Received: 29 March 2013. Accepted: 8 August 2013.

RESEARCH ARTICLE